

Denitrogenation of Piperidine on Alumina, Silica, and Silica-Aluminas: The Effect of Surface Acidity

S. RAJAGOPAL, T. L. GRIMM, D. J. COLLINS, AND R. MIRANDA¹

Department of Chemical Engineering, University of Louisville, Louisville, KY 40292, USA

Received December 17, 1991; revised April 21, 1992

Alumina, silica, and three silica-aluminas having 10, 50 and 90 wt% SiO₂ were prepared and characterized for the total acidity, acid strength distribution, and Brønsted/Lewis acidity. The characterization involved the techniques of ammonia chemisorption, temperature-programmed desorption (TPD), and FT-IR spectroscopy. The effect of surface acidity on denitrogenation selectivity was studied by means of the reactions of piperidine in a continuous-flow fixed-bed reactor operated at atmospheric pressure and 320–340°C. The overall piperidine conversion to various products increases with the total acidity of the catalysts. However, the denitrogenation selectivity depends only on the concentration of Brønsted acid sites, demonstrating the participation of those sites in the deamination mechanism and hence showing evidence for the Hofmann elimination pathway. The other important reactions of piperidine were alkylation, condensation, disproportionation, and dehydrogenation, to yield alkylpiperidines, 2,3,4,5-tetrahydropyridine, pyridine, 1,2,3,4-tetrahydroquinoline, 1,2,3,4-tetrahydro-3-methylquinoline, 5,6,7,8-tetrahydroquinoline, and decahydroquinoline. © 1992 Academic Press, Inc.

INTRODUCTION

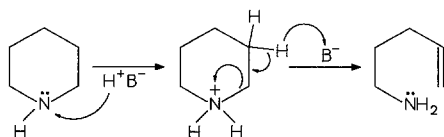
Because efficient removal of nitrogen is of paramount importance in liquid fuel refining, much research effort has been focused on the hydrodenitrogenation (HDN) of model heteroaromatic compounds, such as pyrroles, pyridines, and quinolines (1–3). There is enough evidence that the initial step in the HDN of heteroaromatic compounds over hydroprocessing catalysts like CoMo/ γ -Al₂O₃ and NiMo/ γ -Al₂O₃ is the partial or total hydrogenation of the heterocyclic ring (1). For active hydrogenation catalysts this first step is generally reversible and not rate-limiting. The rate-determining step is usually the opening of the saturated heterocyclic ring, i.e., the scission of the C–N bond. In order to improve the efficiency of the HDN process, much study is being focused on this critical step.

There is some evidence that denitrogenation activity can be improved by utilizing

molybdenum catalysts on strongly acidic supports such as amorphous silica-aluminas or zeolites (1, 2, 4, 5). The reason for this improvement is not clear, although it is possible that the Hofmann elimination mechanism is operative (6) in parallel to the metal-catalyzed hydrogenolysis of the C–N bond. According to such a mechanism (Scheme 1), ring –NH– is protonated by a Brønsted acid site to form substituted quaternary ammonium ion (–NH₂⁺–). Simultaneously, β -H (hydrogen attached to β -carbon atom) is abstracted by a basic site resulting in C–N bond cleavage. If this mechanism were valid, increasing the Brønsted acidity of the molybdenum catalysts would improve their deamination activity by accelerating the Hofmann elimination pathway. More evidence is needed, however, to support this claim.

Previous related work (7–13) dealt with reactions of amines on pure alumina. Most of these studies were performed using primary, secondary, and tertiary acyclic amines except in the work of Sonnemans *et*

¹ To whom correspondence should be addressed.



SCHEME 1. Brønsted acid-catalyzed ring-opening step (Hofmann elimination).

al. (12) and Ledoux and Sedrati (13). These two research groups studied the denitrogenation (DN) of cyclic amines, especially piperidine. Ledoux and Sedrati proposed mechanisms for the transformation of cyclic amines over acidic catalysts like alumina. The participation of Brønsted and Lewis acidity and basicity in the mechanisms of deamination and dehydrogenation were described, but a systematic change of catalyst acidity to obtain more insight into the acidic mechanism was not attempted.

The main objective of this work is to correlate the effect of amount, type, and strength of acidity on denitrogenation selectivity. For this purpose, alumina, a series of silica-aluminas, and silica were prepared, characterized, and tested for the denitrogenation of piperidine, which is an intermediate in the hydrodenitrogenation (HDN) of pyridine. In order to study the activity of acidic sites in the absence of hydrogenolysis sites, the use of transition metal was *deliberately* avoided.

METHODS

Materials

Alumina was prepared as follows: 375 g of $\text{Al}(\text{NO}_3)_3 \cdot 9\text{H}_2\text{O}$ (Fisher Scientific) was dissolved in 1 liter of distilled water. A solution of 200 g of NaOH in 750 ml distilled water was added to the $\text{Al}(\text{NO}_3)_3$ solution at a rate such that no precipitation took place during addition. Then 55 g of HNO_3 in 500 ml of water was added to the above NaAlO_2 solution at a rate of 1 ml/min, under mechanical stirring and at a constant 70°C . The addition of HNO_3 was continued until the pH reached 7.0. The suspension was filtered

and washed with 2 liters of hot 1% NH_4NO_3 solution and 2 liters of distilled water.

Three silica-aluminas ($\text{SiO}_2 : \text{Al}_2\text{O}_3$ weight ratios = 10:90, 50:50, 90:10) were prepared according to established techniques (14). Required amounts of $\text{Na}_2\text{SiO}_3 \cdot 9\text{H}_2\text{O}$ were dissolved in distilled water to obtain a solution of pH 11.8. HNO_3 (3N) was added dropwise until the silicate solution gelled (pH 9.8). The gel was aged for 15 min at 35°C . Requisite amount of $\text{Al}(\text{NO}_3)_3 \cdot 9\text{H}_2\text{O}$ as demanded by $\text{SiO}_2/\text{Al}_2\text{O}_3$ ratio was dissolved in distilled water and was then mixed with silica gel. The mixture was stirred for 10 min and 1:1 NH_4OH was added dropwise until a pH of about 6. NH_4NO_3 solution was added to the above solution and the pH was increased from 6 to 7 using NH_4OH . The precipitate was aged for 2 h at 35°C and for 6 h at 45°C . These samples are designated SA10, SA50, and SA90, respectively.

SiO_2 was obtained from $\text{Na}_2\text{SiO}_3 \cdot 9\text{H}_2\text{O}$ (Fisher Scientific) and dil HNO_3 or H_2SO_4 . All of the above solids were dried at 120°C for 4 h and calcined at 550°C for 12 h. The silica-alumina samples were ion-exchanged three times with NH_4NO_3 and further calcined at 550°C . Ultrahigh pure (UHP) H_2 and He (Air Products) were further purified by passing over *oxygen trap* and molecular sieves (both from Altech Associates). Commercial NH_3 was freed from water by transporting it through a column of solid KOH. Piperidine (Alfa Products) was distilled and stored over a 4A molecular sieve.

BET Surface Area

BET surface areas of these catalysts were determined by nitrogen sorption at -196°C using a conventional high-vacuum gas-handling apparatus equipped with Datameetrics electronic manometer.

Ammonia Chemisorption and Temperature-Programmed Desorption

The NH_3 chemisorption and TPD experimental unit consisted of a quartz reactor (i.d. 8 mm) heated by a tubular furnace, a six-port pulsing valve, and a thermal con-

ductivity detector interfaced to an integrator (Hewlett-Packard Model 3392A). The tubular furnace was regulated by a ramp and soak controller (Lindberg). Chemisorption was performed under helium flow (100 ml/min NTP) by dosing measured pulses of water-free NH_3 (pulse size, 0.646 ml NTP) at 120°C every 15 min until saturation was observed. Before chemisorption, 200 mg of catalyst was pretreated at 500°C under He flow for 1 h. To avoid physisorption of NH_3 , the chemisorption experiments were performed at 120°C. After chemisorption, the catalyst was cooled to 50°C and TPD of NH_3 was carried out by linearly ramping the temperature from 50 to 550°C at 10°C per minute and holding it at 550°C for 20 min. The desorption of NH_3 as a function of temperature (or time) was monitored with the thermal conductivity detector. The TPD spectrum obtained for each catalyst was arbitrarily divided into three segments, viz., 50–200, 200–350, and 350–550°C. The areas under these segments were assigned to NH_3 desorbing from weak, medium, and strong acidic sites, respectively.

FT-IR Spectra of Adsorbed Pyridine

A Perkin-Elmer FT-IR spectrophotometer (Model 1720) and computer data station were employed to collect and process infrared spectra. A diffuse reflectance IR cell (Spectra Tech) equipped with an environmental chamber capable of providing the catalyst sample with high vacuum, gas flow, and high temperature (to 600°C) was used for the IR experiments. The catalysts were pretreated at 500°C under He (5 ml/min NTP) for 1 h in the DRIFT cell and cooled to 200°C before a blank spectrum was obtained. Pyridine was then adsorbed on the catalysts at 200°C until saturation, by upstream injection of 2 μl of dry pyridine. The IR spectra of the adsorbed pyridine was recorded at 200°C after allowing 1 h for the desorption of loosely bound pyridine from the surface of the catalyst. The reflectance spectra were converted to $-\log(\text{reflectance})$, which is equivalent to *ab-*

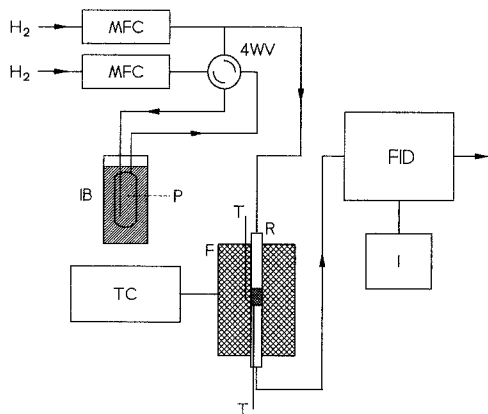


FIG. 1. Experimental setup for activity studies. MFC, mass flow controllers; 4WV, four-way valve; R, quartz reactor; T, thermocouples; F, furnace; TC, temperature controller; IB, ice bath; P, piperidine; FID, flame ionization detector; and I, integrator.

sorbance in transmission spectroscopy, by means of software available in the spectrophotometer. The integrated areas under the pyridine absorption bands LPy (1449 cm^{-1}) and BPy (1545 cm^{-1}) were computed using the Micro-Search program supplied by Sprouse Scientific Systems, Inc. The limits chosen for integration of LPy and BPy bands were 1420–1470 and 1515–1565 cm^{-1} , respectively.

Activity Studies

The reaction was performed at atmospheric pressure in a continuous-flow fixed-bed quartz reactor with an internal diameter of 4.5 mm (Fig. 1). An insulated cylindrical metal block provided with cartridge heaters was used as a furnace. The isothermicity of the furnace was confirmed by employing a moving thermocouple. The temperature of the catalyst was regulated by a type K thermocouple which was positioned close to the catalyst bed in the axial direction. The inlet and effluent lines were wrapped with electrical heating tape (temperature: $120 \pm 5^\circ\text{C}$) to avoid condensation of reactants and products. The catalyst sample (100 mg; particle diameter $<150 \mu\text{m}$) was pretreated in flowing H_2 (30 ml/min NTP) at 500°C before test-

TABLE I
BET Surface Areas and Acidic Properties of the Catalysts

	Alumina	SA10	SA50	SA90	SiO ₂
Surface area (m ² /g)	150	264	306	382	311
Acidity (mmol/g)					
Total	0.304	0.503	0.438	0.162	0.001
Weak	0.077	0.120	0.128	0.046	—
Medium	0.149	0.274	0.228	0.075	—
Strong	0.078	0.109	0.082	0.041	—

ing with the piperidine reaction at two temperatures (320 and 340°C). The feed consisted of 0.32 mol% piperidine vapor in hydrogen (30 ml/min NTP). This concentration was stable with time and was verified by gas chromatography. To obtain such a concentration, 9 ml/min of hydrogen was saturated with piperidine at 0°C, and was diluted with 21 ml/min of pure hydrogen. The flow rates were maintained constant by means of mass flow controllers (see Fig. 1). The reaction was carried out continuously for 24 h over each catalyst, i.e., 12 h at each temperature. The conversion values reported here are those measured at steady state, when the deactivation rate was negligible. Homogeneous reactions were not observed under the conditions of these experiments.

Product Analysis

The product was analyzed by an on-line gas chromatograph (HP 5890A) furnished with a 10-port sampling valve and two separate columns, viz. (10% Carbowax 1500 + 1% KOH) on Chromosorb W and *n*-octane/Porasil C. The analysis technique allowed the separation of C₁–C₅ hydrocarbons and nitrogen-containing compounds in a single run (15). The amine products were identified separately with GC–MS (HP Model 5890 series II GC and HP Model 5970B MS) using a crossbonded 100% dimethyl polysiloxane capillary column (60 m long, 0.25 mm i.d., and 2.00 μm *df*).

RESULTS AND DISCUSSION

Table I reports for each of the five catalysts: (i) the measured BET surface area, (ii) the total acidity determined from dynamic NH₃ chemisorption, and (iii) the strength distribution of acidity among weak, medium, and strong sites, calculated from the TPD profiles shown in Fig. 2. The total acidity, which is expressed as millimoles of NH₃ per gram of catalyst, reached a maximum for SA10. Since the acidity of silica was negligibly low, its acidity distribution was not determined.

The TPD results of Fig. 2 could be precisely reproduced when the catalysts were consistently pretreated. The mass balance of adsorbed and desorbed NH₃ was within

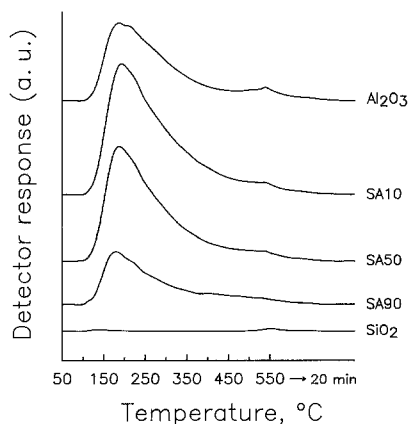


FIG. 2. Temperature-programmed desorption of ammonia profiles for alumina, silica, and silica-aluminas.

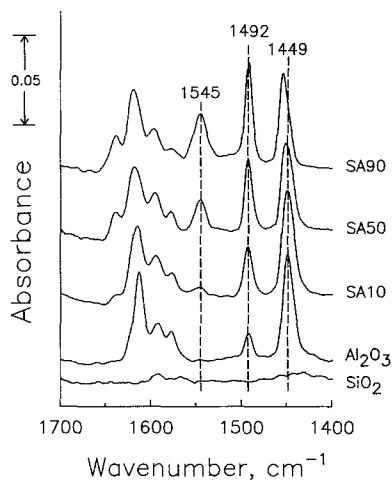


FIG. 3. Diffuse reflectance infrared spectra of adsorbed pyridine at 200°C.

experimental error (3%) and no residual NH_3 was detected upon heating the catalysts to higher temperature ($>550^\circ\text{C}$) after the TPD experiments. Thus, the total acidity obtained by this method was considered quantitative.

According to the classical developments of Ehrlich (16) and Redhead (17) for single crystals and Cvetanovic and Amenomiya for powders (18), the TPD profiles indicate a broad distribution of binding strength of NH_3 and hence of acid strength of the solids. The distribution was arbitrarily divided into three regions (50–200, 200–350, and 350–550°C) to provide a measure of weak, medium, and strong acid sites, respectively. Table 1 indicates that irrespective of the composition, in all three silica-aluminas and alumina, 24–30% of all acid sites are weak, 45–55% are medium, and 19–26% are strong. The nature of this acidity was then determined from the results of infrared spectroscopy of adsorbed pyridine (Fig. 3).

Pyridine is known to chemisorb on oxides mainly in two modes: on Lewis acid sites (coordinatively unsaturated or electron-pair acceptor sites) by coordination of nitrogen lone pair of electrons and on Brønsted acid sites by transfer of proton from the site to

nitrogen. In addition, infrared-perceptible physisorbed and H-bonded pyridines have also been reported (19). In the present work, the Brønsted and Lewis sites were quantified from the amount of pyridine adsorbed in the first two modes. It has been well documented (20, 21) that the band at $\sim 1450\text{ cm}^{-1}$ is characteristic of pyridine adsorbed on Lewis acid sites (LPy), the one at $\sim 1545\text{ cm}^{-1}$ corresponds to Brønsted acid sites (BPy), and the one at $\sim 1490\text{ cm}^{-1}$ is a combination band. Figure 3 shows that alumina contains only Lewis acid sites, whereas silica-aluminas contain both Lewis and Brønsted sites. Brønsted acidity increases with silica content reaching a maximum value for SA90.

A close look at the band corresponding to Lewis sites (ν_{19b} band) reveals a gradual shift to higher frequency as silica/alumina ratio increases, i.e., from 1449 cm^{-1} for Al_2O_3 to 1455 cm^{-1} for SA90. A possible reason for this shift is the change in coordination environment of aluminum ion, an effect that has been documented in silica-aluminas (22). Pyridine adsorbed on octahedrally coordinated Al cations exhibits a band at 1615 cm^{-1} and that on tetrahedral Al at 1624 cm^{-1} (23). Tetrahedral aluminum species ($\text{Al}_{\text{cus}}^{\text{IV}}$) are more acidic (24) than octahedral aluminum ($\text{Al}_{\text{cus}}^{\text{VI}}$) and thus interact with pyridine more strongly causing the band shift to higher frequency. Therefore our results indicate that in silica-aluminas the population of tetrahedral Al species increases with silica content (Fig. 3), in agreement with other sources (22). Adsorption on pure silica at relatively low temperature, for example 25°C , is known to produce two bands at 1447 and 1599 cm^{-1} (not appearing here), corresponding to pyridine adsorbed on surface silanol groups via H-bonding (25). However, at 200°C pyridine does not absorb on silica. Hence, ammonia chemisorption, TPD of NH_3 , and FT-IR spectroscopy of adsorbed pyridine suggest that silica has no acidity of reasonable strength to catalyze the reactions of piperidine.

The quantification of Brønsted and Lewis

TABLE 2
Piperidine Conversions over γ -Alumina and
Amorphous Silica-Aluminas

Catalysts	Reactions	Percentage	
		320°C	340°C
Al ₂ O ₃	Denitrogenation ^a	0.13	0.31
	Dehydrogenation to pyridine	6.01	11.1
	Other reactions ^b	3.03	6.29
	Total conversion	9.17	17.7
SA10	Denitrogenation	1.63	3.41
	Dehydrogenation to pyridine	4.82	9.38
	Other reactions	4.85	21.9
	Total conversion	11.3	34.7
SA50	Denitrogenation	1.87	4.31
	Dehydrogenation to pyridine	4.41	9.20
	Other reactions	2.87	15.2
	Total conversion	9.15	28.7
SA90	Denitrogenation	2.36	5.36
	Dehydrogenation to pyridine	2.88	5.60
	Other reactions	1.68	4.74
	Total conversion	6.92	15.7

^a Percentage piperidine conversion to C₁-C₅ hydrocarbons and ammonia. Estimation is based on hydrocarbon formation only since NH₃ cannot be detected by FID.

^b These include condensation, cyclization, alkylation, etc.

acid sites from IR spectra needs the molar absorptivities for BPy and LPy absorption (ν_{196}) bands. The absolute values for these bands are difficult to measure and hence are usually not reported in the literature. Instead, most research groups have reported the relative *molar absorptivities* measured by indirect methods. For example, Refs. (26-30) give $\epsilon_{1450}^L/\epsilon_{1545}^B$ the value of 0.9 ± 0.1 , 1.08 ± 0.09 , 1.1, 1.54, and 8.8, respectively. In the present study, the relative molar absorptivity has been taken as unity in order to calculate the ratio of Brønsted/Lewis acidity. It was thus found that the ratio of Brønsted to Lewis acidity increases with SiO₂ content, in agreement with other works (31).

The acidic characteristics thus determined were then correlated with the activity and selectivity for the piperidine reaction. The observed reaction products were divided into three groups: (i) hydrocarbons, obtained by denitrogenation, (ii) pyridine, produced by dehydrogenation, and (iii) other nitrogen-containing compounds, formed as a result of condensation, alkyl-

ation, etc. (Table 2). Hydrocarbons include paraffins (C₁-C₅), olefins (C₂-C₅), and diolefins (C₅). The majority of these are C₅'s indicating that further (hydro)cracking is not very facile under these reaction conditions. The concentration of nitrogen-containing products (group (iii) above) are in this order: 5,6,7,8-tetrahydroquinoline > alkylpiperidines > 2,3,4,5-tetrahydropyridine > 1,2,3,4-tetrahydroquinoline > decahydroquinoline > 5,6,7,8-tetrahydro-3-methylquinoline. The yields have been indicated in Table 2 as conversion of piperidine into each one of these groups of products, including also the total piperidine conversion. Silica is excluded from the table because it exhibited no activity.

As shown in Fig. 4, the piperidine conversion at 320 and 340°C is related to the total number of acid sites. Therefore, it can be concluded that both Brønsted and Lewis acid sites are effective in transforming piperidine to various products. However, when turnover numbers (piperidine molecules reacted per acid site per second) are plotted against weight fraction of SiO₂ (Fig. 5), the correlation deviates for silica-rich catalysts like SA90, on which the proportion of Brønsted sites is higher. This deviation may be due to higher intrinsic activity of Brønsted acid sites. In fact, it has been suggested that Brønsted acid sites are much more active than Lewis sites for skeletal isomerization of hydrocarbons (32).

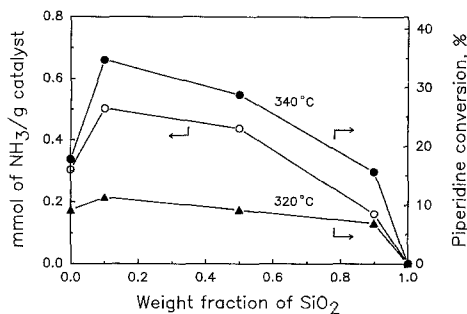


FIG. 4. Total acidity and piperidine conversions at atmospheric pressure and 320 and 340°C.

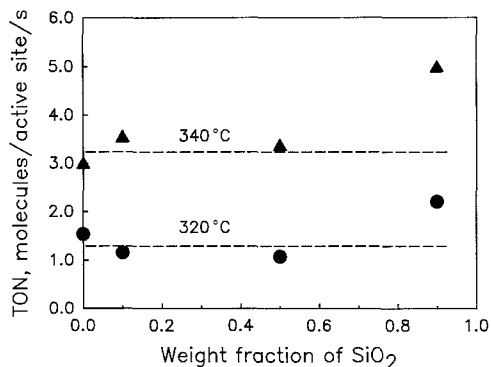
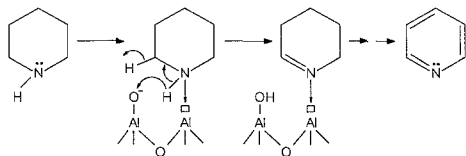


FIG. 5. Turnover number (TON) versus weight fraction of SiO_2 . (TON, number of piperidine molecules reacted per acid site per second).

The conversion of piperidine to pyridine by dehydrogenation is 6.01% at 320°C on $\gamma\text{-Al}_2\text{O}_3$ and this value decreases with increase in silica content, reaching 2.88% for SA90. A similar trend is observed at 340°C. The following mechanism of dehydrogenation provides an interpretation of these results. The first step of the dehydrogenation is the abstraction of hydrogen attached to nitrogen followed by the loss of hydride ion to form tetrahydropyridine. These steps are achieved by the chemisorption of piperidine through nitrogen lone pair on Lewis acid sites and by the abstraction of hydrogen by basic groups like $\sigma\text{-O}^-$ which are present on these catalysts (Scheme 2). Tetrahydropyridine undergoes further dehydrogenation to dihydropyridine and finally to pyridine. Being a relatively stable intermediate, tetrahydropyridine appears in the product stream. However, dihydropyridine is not detected since it immediately loses two hy-



SCHEME 2. Mechanism of dehydrogenation involving acid-base bifunctional catalysis.

drogens to form pyridine which is thermodynamically more stable. Alumina, which contains Lewis acid sites and $\sigma\text{-O}^-$ groups, catalyzes dehydrogenation of piperidine by acid-base pairs. Silica-aluminas, which contain additional Brønsted acidity, catalyze other reactions involving the intermediates of dehydrogenation products. As a result, the pyridine formation is lower on silica-aluminas than alumina. Thus, the cooperation of Lewis acidic and basic sites, which is maximum for alumina, is responsible for high pyridine formation.

It has been proven that gas-phase hydrogen is not participating during piperidine reactions (13). However, our product distribution suggests that hydrogen transfer reactions are occurring; i.e., the protons and hydrides liberated during the acidic dehydrogenation are consumed by the unsaturated compounds like olefins.

The heavy nitrogen-containing products detected also indicate that alkylation of partially dehydrogenated piperidine with hydrocarbons is highly favored on these catalysts. The absence of *n*-pentylamine and *n*-pentenylamine (ring-opening products of piperidine) emphasizes the fact that deamination of aliphatic amines is much faster than cyclic amines. Disproportionation or transalkylation of piperidine to *N-n*-pentylpiperidine was not observed in these experiments, although they are known to occur at high pressure (12).

Finally, the piperidine conversion to hydrocarbons does not correlate with total acidity, but it does with Brønsted acidity. The plots of denitrogenation activity and the percentage Brønsted sites versus weight fraction of SiO_2 (Fig. 6) give a clear indication that the denitrogenation reaction is strongly dependent on Brønsted sites, in accordance with the classical Hofmann elimination mechanism. From the denitrogenation activity of alumina, it is evident that pure Lewis acidity does not catalyze the denitrogenation of piperidine at $<340^\circ\text{C}$. The observed residual denitrogenation activity is caused by the weak Brønsted acidity

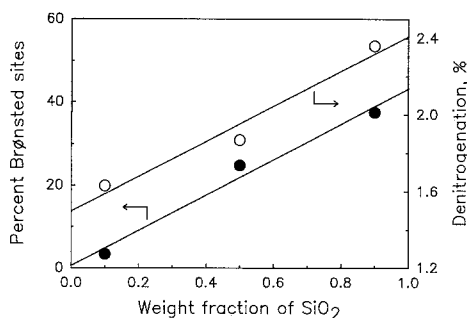


FIG. 6. Percentage Brønsted acid sites and piperidine denitrogenation at 340°C.

($\sigma\text{-O-H}^{\delta+}$) present on alumina (33, 34). Tanabe (35) and Pines (36) have suggested that traces of moisture around alumina generate the Brønsted acidity. As in the dehydrogenation reaction, the basic sites play an important role also during denitrogenation since they are responsible for the $\beta\text{-H}$ abstraction needed to complete the ring-opening step (Scheme 1). Since both acidic and basic sites interact with the substrate in a concerted fashion, the denitrogenation activity is strongly dependent on the Brønsted sites. In addition to E2-type elimination, attack at C_{α} atom by bases like NH_3 , *n*-pentylamine, piperidine, or $\sigma\text{-O}^-$, followed by C–N bond cleavage (nucleophilic ring opening), may be possible and hence cannot be ruled out.

It was also noted that the reaction of pyridine over alumina, silica, and silica-aluminas did not proceed to any appreciable extent at $\leq 400^\circ\text{C}$. This result shows that acidic sites (Brønsted or Lewis) are not able to effect the denitrogenation of *heteroaromatics*. Such a result is in agreement with the Hofmann elimination mechanism which demands the sp^3 nature of C_{β} atom and availability of $\beta\text{-H}$.

CONCLUSIONS

Evidence that acid sites (in concerted action with basic sites) catalyze the reactions of piperidine under hydrotreatment conditions has been provided. Such reactions can

be classified into: (i) denitrogenation via E2-type elimination yielding hydrocarbons, (ii) dehydrogenation catalyzed by acid–base pairs producing pyridine, and (iii) condensation/alkylation generating larger amine molecules. It was shown that Lewis acidity catalyzes dehydrogenation and condensation, but not denitrogenation. Thus, a small denitrogenation activity shown by alumina is probably due to the presence of weak Brønsted acid sites. On the other hand, Brønsted acidity present on silica-aluminas catalyzes denitrogenation, a result that provides evidence for the classical Hofmann elimination mechanism. The overall conversion of piperidine is in direct relationship with the total (Brønsted and Lewis) acidity.

ACKNOWLEDGMENTS

We acknowledge the financial support of the Department of Energy (Grant DE-FG22-89PC89771), the National Science Foundation (Grant RII-8610671), and the Commonwealth of Kentucky (EPSCoR Program).

REFERENCES

- Ledoux, M. J., in "Catalysis, Specialist Periodical Reports" (G. C. Bond and G. Webb, Eds.), Vol. 7, p. 125. The Royal Society of Chemistry, London, 1985; and patents cited therein.
- Ho, T. C., *Catal. Rev. Sci. Eng.* **30**, 117 (1988).
- Shabtai, J., Yeh, G. J. C., Russell, C., and Oblad, A. G., *Ind. Eng. Chem. Res.* **28**, 139 (1989); and references cited therein.
- Henseley, A. L., Jr., Tait, A. M. Miller, J. T., and Nevitt, T. D., U.S. Patent 4,406,779 (1983).
- Miller, J. T., and Hineman, M. F., *J. Catal.* **85**, 117 (1984).
- Nelson, N., and Levy, R. B., *J. Catal.* **58**, 485 (1979).
- Catry, J. P., and Jungers, J.-C., *Bull. Soc. Chim. Fr.*, 2317 (1964).
- Pavsek, J., Tyrpekl, J., and Machová, M., *Coll. Czech. Chem. Commun.* **31**, 4108 (1966).
- Firky Ebeid, M., and Pavsek, J., *Coll. Czech. Chem. Commun.* **35**, 2166 (1970).
- Hogan, P., and Pavsek, J., *Coll. Czech. Chem. Commun.* **38**, 1513 (1973).
- Beránek, L., and Kraus, M., in "Comprehensive Chemical Kinetics" (C. H. Bamford and C. F. H. Tipper, Eds.), Vol. 20, p. 263. Elsevier, Amsterdam, 1978.
- Sonnemans, J., Neyens, W. J., and Mars, P., *J. Catal.* **34**, 230 (1974).
- Ledoux, M. J., and Sedrati, M., *J. Catal.* **83**, 229 (1983).

14. Magee, J. S., and Blazek, J. J., in "Zeolite Chemistry and Catalysis" (J. B. Rabo, Ed.), Am. Chem. Soc. Monograph 171, p. 615, Am. Chem. Soc., Washington, DC, 1976.
15. Rajagopal, S., Grimm, T. L., Collins, D. J., and Miranda, R., *Anal. Lett.* **23**, 649 (1990).
16. Ehrlich, G., *J. Appl. Phys.* **32**, 4 (1961); *Adv. Catal. Relat. Subj.* **14**, 271 (1963).
17. Redhead, P. A., *Vacuum* **12**, 203 (1962).
18. Cvetanovic, R. J., and Amenomiya, Y., *Adv. Catal. Relat. Subj.* **17**, 103 (1967); *Catal. Rev.* **6**, 21 (1972).
19. Ward, J. W., in "Zeolite Chemistry and Catalysis" (J. B. Rabo, Ed.), Am. Chem. Soc. Monograph 171, p. 118. Am. Chem. Soc. Washington, DC, 1976.
20. Tanabe, K., in "Catalysis: Science and Technology" (J. R. Anderson and M. Boudart, Eds.), Vol. 2, p. 231. Springer-Verlag, Berlin, 1981.
21. Kung, M. C., and Kung, H. H., *Catal. Rev. Sci. Eng.* **27**, 425 (1985).
22. Leonard, A., Suzuki, S., Fripiat, J. J., and De Kimpe, C., *J. Phys. Chem.* **68**, 2608 (1964).
23. Connell, G., and Dumesic, J. A., *J. Catal.* **102**, 216 (1986).
24. Knözinger, H., in "Catalysis by Acids and Bases" (B. Imelik, C. Naccache, G. Goudurier, Y. B. Taarit, and J. C. Vardine, Eds.), p. 111. Elsevier, Amsterdam, 1985.
25. Parry, E. P., *J. Catal.* **2**, 371 (1963).
26. Matulewicz, E. R. A., Kerkhof, F. P. J. M., Moulijn, J. A., and Reitsma, H. J., *J. Colloid Interface Sci.* **77**, 110 (1980).
27. Ward, J. W., *J. Catal.* **11**, 271 (1968).
28. Hughes, T. R., and White, H. M., *J. Phys. Chem.* **71**, 2192 (1967).
29. Lefrancois, M., and Malbois, G., *J. Catal.* **20**, 350 (1971).
30. Basila, M. R., Katner, T. R., and Rhee, K. H., *J. Phys. Chem.* **68**, 3197 (1964).
31. Schwarz, J. A., Russell, B. G., and Harnsberger, H. F., *J. Catal.* **54**, 303 (1978).
32. Benesi, H. A., and Winkvist, B. H. C., *Adv. Catal.* **27**, 97 (1978).
33. Peri, J. B., *J. Phys. Chem.* **69**, 231 (1965).
34. Dunken, H., and Fink, P., *Z. Chem.* **5**, 432 (1965).
35. Tanabe, K., "Solid Acids and Bases." Academic Press, New York, 1970.
36. Pines, H., *J. Catal.* **78**, 1 (1982).